# LANDSLIDE DETECTION WITH MULTI-DIMENSIONAL HISTOGRAM EQUALIZATION FOR MULTISPECTRAL REMOTELY SENSED IMAGERY

Cheng-Feng Lin [a] and Hsuan Ren [b]

[a] Master student, Graduate Institute of Space Science,
National Central University, No.300, Jhongda Rd., Jhongli City, 32001, Taiwan
Tel: +886-3-4227151-57673; Fax: +886-3-4255535
E-mail: chenfeng1010@gmail.com

[b] Associate Professor, Center for Space and Remote Sensing Research,
National Central University, No.300, Jhongda Rd., Jhongli City, 32001, Taiwan
Tel: +886-3-4227151-57673; Fax: +886-3-4255535
Email: hren@csrsr.ncu.edu.tw

**KEY WORDS:** Landslides, NDVI, multi-dimensional histogram equalization, multispectral, remote sensing

**Abstract:** Landslides are serious natural hazards. They usually cause significant properties damage and sometimes also fatalities. For reconstruction and rescue purposes, landslide detection is very important. Normalized Difference Vegetation Index (NDVI) is widely used for this purpose. If NDVI significantly decreases within a short period, that area will be considered as landslide candidate. However, remote sensing images always contain atmospheric effects which affect the NDVI estimation. In this study, we propose a multi-dimensional histogram equalization algorithm as a pre-process step. It modifies multispectral images collected under different atmospheric conditions to have similar spectrum for the same land cover. A set of SPOT images is adopted for experiments and preliminary results show the proposed method can reduce the misclassification rate.

## 1. INTRODUCTION

Optical remote sensing satellites record tens to hundreds co-registered images of the earth surface with different wavelengths from visible and infrared ranges. The spectral information provided by multispectral and hyperspectral images is widely used to analyze of surface contents [1-3]. Among various applications, the detection of the surface changes is one of the most important applications in remote sensing technology. By comparing two remote sensing images collected at different time from the same location, the surface changes can be detected. The detection of the surface changes can be conducted by comparing the spectrum. However, not all changes in spectrum are caused by surface changes, atmospheric factors and solar illumination would also affect the radiation spectrum. In this case, the surface changes may be overestimated. Therefore, we have to calibrate the radiometric effect before comparing the spectrum. There are two types of radiometric calibration: absolute and relative calibration. For absolute radiometric calibration, several atmospheric and solar parameters are needed with the collection of the multispectral images, so that the atmospheric effects can be removed. But these parameters are usually not provided which makes this procedure hard to complete. On the other hand, relative radiometric calibration is a good choice to modify the effect caused by atmospheric and solar illumination, so the two images will have similar condition.

Two widely used relative radiometric calibration methods are proposed in the past and they are mean and variance method (MV) [4], whitening/dewhitening transform (WD) [4,5]. Since the images are collected from the same sensor with the same spectral bands, the statistical properties should be similar. The MV method assumes the first and second statistical data should be the same if there are no atmospheric and solar effects, so the mean and variance of one image collected at a specific time is adjusted to match those of another image with a linear transformation equation. The WD transform can be viewed as multispectral version of the MV method. Instead of match the mean and variance of each spectral band, it matches the mean vector and the covariance matrix of all bands together. Whitening is an important step for multi-dimensional data by transforming the data to zero mean and identity covariance matrix, therefore, it can remove the correlation between the image bands. And then the dewhitening step applies new mean vector and covariance matrix to match the statistics of the second multispectral images. However, these methods are all linear transformation which did not model the nonlinearity in atmospheric effect.

In this paper, we propose a multi-dimensional histogram equalization (MHE) algorithm as a pre-process step. It modifies multispectral images collected under different atmospheric conditions to have similar spectrum for the same land cover. The MHE transform matches the multidimensional Cumulated Distribution Function (CDF) of all bands nonlinearly which may accommodate the nonlinear atmospheric effect. After this step, the probability of overestimated surface changes may be reduced. A set of SPOT images is adopted for experiments and preliminary results show the proposed method can reduce the misclassification rate.

## 2. MEAN AND VARIANCE METHOD (MV)

Let $X_1$ is a multispectral image with $L$ bands and $N$ pixels of each band. The data set can express as an $L \times N$ matrix. The mean ( $\mu_i$ ) and variance ( $\sigma_i^2$ ), are calculated for each band:

$$\mu_i = \frac{1}{N}\sum_{n=1}^{N} X_1(i,n) \tag{1}$$

$$\sigma_i^2 = \frac{1}{N}\sum_{n=1}^{N} (X_1(i,n) - \mu_i)^2 \tag{2}$$

To transform $X_1$ to have the same mean and variance with another one linearly, we first normalize the data to zero mean and unity variance, and then match the original matrix $X_1$ to a new one $\hat{X}_1$ , as shown in Eqs. (3), (4) and (5). After this linearly transformation for each band, both image sets will have the same mean and variance in all bands for surface changes detection.

$$\frac{1}{N}\sum_{n=1}^{N} \left(\frac{x_{in} - \mu_i}{\sigma_i}\right)^2 = 1 \tag{3}$$

$$\frac{1}{N}\sum_{n=1}^{N}\left(\frac{x_{in}-\mu_i}{\sigma_i}\right)=0 \quad (4)$$

$$\hat{X}_1=\frac{\sigma_1}{\sigma_2}(X_1-\mu_1)+\mu_2 \quad (5)$$

**WHITENING/DEWHITENING TRANSFORM (WD)**

The WD transform is a multi-dimensional version of the MV method. It matches the mean vector and covariance matrix of all bands together. The whitening step eliminates the correlation of the bands. Let $X$ represents the image cube collected at one time, and then subtract the mean vector of $X$ from itself to have zero mean data $\widetilde{X}=X-\mu\cdot 1^T$, where $\mu=\frac{1}{N}\sum_{n=1}^{N}X_n$ and $1=[11...1]^T$. To transform data with identity covariance matrix, we first compute the eigenvalues $\{\lambda_i\}$( $i$ = 1, 2, …, $L$) and the corresponding eigenvectors $\{v_i\}$($i$ = 1, 2, …, $L$) of the covariance matrix $\Sigma=\widetilde{X}\widetilde{X}^T$. Based on the properties, decompose $\Sigma$ to an identity matrix:

$$\Lambda^{-1/2}V^T\Sigma V\Lambda^{-1/2}=I \quad (6)$$

where $V$=[$v_1v_2…v_L$] is the eigenvector matrix and $\Lambda$=$diag\{\lambda_i\}$($i$ = 1, 2, …, $L$) is a diagonal matrix composed by the eigenvalues. Finally, we let the whitening matrix $A$ as

$$A=V\Lambda^{-1/2}, \quad (7)$$

so that $A^T\Sigma A=I$. After whitening process, the new image cube $Y=A^T(X-\mu\cdot 1^T)$ will have zero mean vector and identity covariance matrix. For the dewhitening process, let $A_z$ be the whitening matrix and $\mu_z$ be the mean vector of another image cube $Z$ , we can transform $X$ to target image $\hat{Z}$ from the following equations.

$$A_z^T(\hat{Z}-\mu_z\cdot 1^T)=Y \quad (8)$$

$$\hat{Z}=\mu_z\cdot 1^T+(A_z^T)^{-1}A^T(X-\mu\cdot 1^T) \quad (9)$$

**MULTIDIMENSIONAL HISTOGRAM SPECIFICATION TRANSFORM (MHS)**

The algorithm of multidimensional PDF matching presented in [6] is shown as follow:

(1) Initialize source ($X_1$) and target ($X_2$) images, both with $L$ bands and $N$ pixels of each band and set $s$←1, $X_1(0)$←$X_1$

(2) Choose a rotate matrix $R$

(3) **repeat**

rotate $X_1$ and $X_2$: $X_{1\_R}(s)$←$RX_1(s-1)$ and $X_{2\_R}$←$RX_2$

(4) project $P_1(X_{1\_R}(s))$ on the $L$ axes to get the marginal density functions $P_{1\_m}(X_{1\_R}(s))$, $m$ = 1, 2, …, $L$

(5) match the marginal density functions of $X_1$ to $X_2$'s for each band

(6) rotate and transform back to the spectral distribution: $X_1(s)$←$R^{-1}X_{1\_r}(s)$

(7) $s \leftarrow s + 1$, back to (3)

(8) **until** exceeds the convergence criterion

The convergence criterion is the PDF of $X_1$ may not be changed at one of the iterations, i.e. the PDF of $X_1$ is almost the same with $X_2$'s. The rotate matrix $R$ is constructed by multiplying separate rotate matrices as

$$R = R_1 \cdot R_2 \cdot \ldots \cdot R_n \tag{14}$$

where $n = C_2^L$. For $L = 4$, the separate matrices are:

$$R_1 = \begin{bmatrix} \cos\theta_1 & \sin\theta_1 & 0 & 0 \\ -\sin\theta_1 & \cos\theta_1 & 0 & 0 \\ 0 & 0 & 1 & 0 \\ 0 & 0 & 0 & 1 \end{bmatrix}, R_2 = \begin{bmatrix} 1 & 0 & 0 & 0 \\ 0 & \cos\theta_2 & \sin\theta_2 & 0 \\ 0 & -\sin\theta_2 & \cos\theta_2 & 0 \\ 0 & 0 & 0 & 1 \end{bmatrix}, \ldots, R_6 = \begin{bmatrix} \cos\theta_6 & 0 & 0 & \sin\theta_6 \\ 0 & 1 & 0 & 0 \\ 0 & 0 & 1 & 0 \\ -\sin\theta_6 & 0 & 0 & \cos\theta_6 \end{bmatrix} \tag{15}$$

The rotate angles are randomly selected in the interval [0, 2π).

The flowchart is shown in Figure 1.

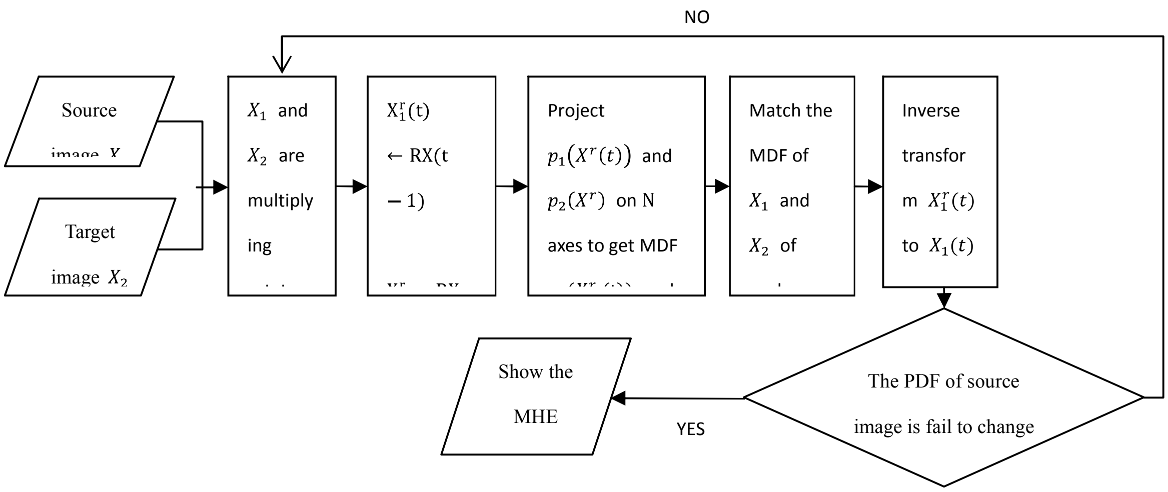


**Figure 1:** Flowchart of MHE

## 3. EXPERIMENT& RESULTS

The 921 earthquake severely damaged the Central Cross-Island Highway and caused massive landslides. Therefore, we selected the area of Ku-Kuan Reservoir in the Central Cross-Island Highway of the SPOT-2 multispectral data. The channels are in the green$(0.5\mu m - 0.59\mu m)$, red$(0.61\mu m - 0.68\mu m)$ and NIR$(0.79\mu m - 0.89\mu m)$ region. These images collected between after and before of the earthquake are at the time of 01 April 1999 and 15 October 1999, respectively.

(a) (b)

**Figure 2:** Ku-Kuan Reservoir in the Central Cross-Island Highway of the SPOT-2 images used for experiment (a) Image acquired in 01 April 1999 (b) Image acquired in 15 October 1999.

Fig.2 (b) is selected as source image to match the multidimensional histogram in Fig.2 (a). The MHE result is shown in Fig 3 and the spectral color is much similar to Fig 2(a).

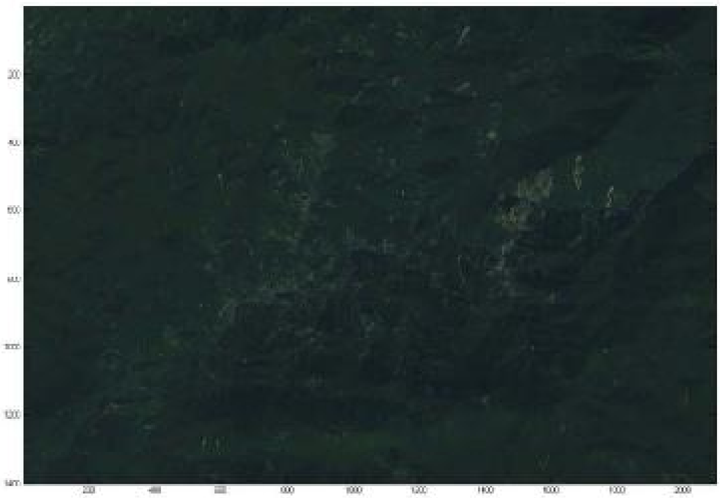

**Figure 3:** The MHE result.

After the calibration, k-means cluster is adopted for land cover classification in Fig 2(a) and Fig 3. Figure 4 (a) is the classification map of Fig 2 (a). We can see that after the earthquake, there was occurred massive landslide at the hillside. Figure 4 (b) is the NDVI image of after earthquake, which can help us to determine where landslides occur. Compare Figure 4 (c) and (d), the yellow regions are landslide candidates. As expected, after image pre-processing, the land slide caused by earthquake can be identified more clearly.

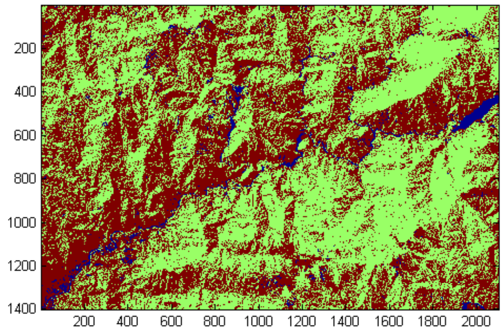


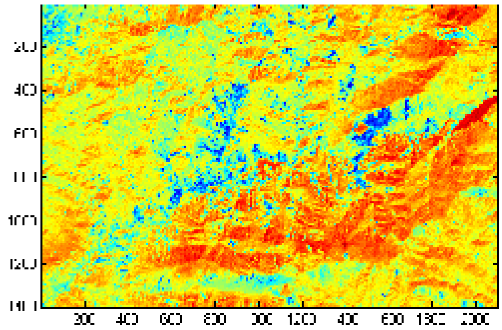

(a) (b)

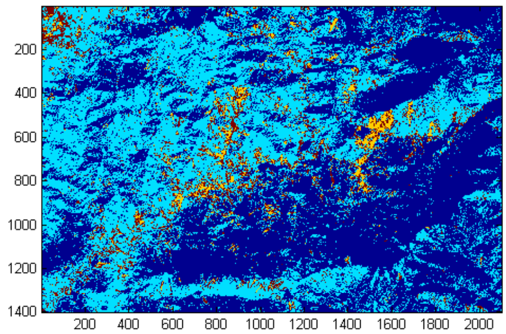


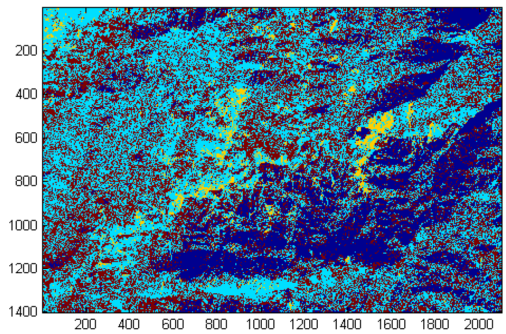


(c) (d)

**Figure 4:** (a) classification map of fig 2(a); (b) NDVI image of fig 2(b); (c) classification map of fig 2(a), (d) classification map fig 3.

## 4. CONCLUSIONS

Since the ground truth of Ku-Kuan Reservoir in the Central Cross-Island Highway is not available, therefore in this experiment we compare the result of classification between original and pre-processing image. As expected, the classification results have been improved. As the classification approach, k-means cluster is not stable, therefore we may investigate more classification algorithms as future works. Furthermore, we can include NDVI threshold or spatial information of DEM to increase detection accuracy.

## REFERENCES:

1. C.I. Chang, Hyperspectral Imaging: Techniques for Spectral Detection and Classification, *New York: Kluwer*,

2003.

2. J.A. Richards and X.P. Jia, *Remote Sensing Digital Image Analysis: An Introduction*, 4th edition, Spinger, 2005.
3. T.M. Lillesane, R.W. Kiefer and J.W. Chipman, *Remote Sensing and Image Interpretation*, 5th edition, Wiley, 2003.
4. R. Mayer, F. Bucholtz, D. Scribner, and M. Kruer, A Family of Spectral Target Signature Transforms: Relationship to the Past, New Transforms, and Sensitivity Tests, *IEEE Trans. Geosci. Remote Sensing Lett.*, vol. 1,pp.26-30, Jan. 2004.
5. R. Mayer and F. Bucholtz, Object Detection by Using “Whitening/Dewhitening” to Transform Target Signature in Multitemporal Hyperspectral and Multispectral Imagery, *IEEE. Trans. Geosci. Remote Sensing*, vol. 40, no. 4, pp.831-840, Apr. 2002.
6. S. Inamdar , F. Bovolo , L. Bruzzone and S. Chaudhuri "Multidimensional probability density function matching for preprocessing of multitemporal remote sensing images", IEEE Trans. Geosci. Remote Sens., vol. 46, pp.1243 2008